



Learning from pathophysiological aspects of COVID-19 clinical, laboratory, and high-resolution CT features: a retrospective analysis of 128 cases by disease severity

Sameh Mostafa Azab¹ · Ashraf Anas Zytoon¹ · Zeinab Abdel Aziz Kasemy² · Suzan Fouad Omar¹ · Suzy Fayez Ewida³ · Karim Ayman Sakr⁴ · Tarek Fawzy Abd Ella¹

Received: 30 September 2020 / Accepted: 23 November 2020 / Published online: 8 January 2021
© American Society of Emergency Radiology 2021

Abstract

Background The classic chest CT imaging features of COVID-19 pneumonia have low specificity due to their similarity with a number of other conditions. So, the goal of the present study is to learn from the pathophysiology of COVID-19 clinical features, laboratory results, and high-resolution CT manifestations in different stages of disease severity to provide significant reference values for diagnosis, prevention, and treatment.

Methods This was a multicentered study that included 128 patients. Demographic, clinical, and laboratory data, in addition to chest HRCT findings, were evaluated. According to chest HRCT features, radiologic scoring were grade 1 and 2 for mild grades of the disease, 3 and 4 for moderate grades of the disease, and 5 and 6 for severe grades of the disease.

Results Patient clinical symptoms ranged between fever, dry cough, muscle ache (myalgia)/fatigue, dyspnea, hyposomnia, sore throat, and diarrhea. Lymphocytes and WBCs were significantly lower in patients with severe COVID-19. A significant negative correlation was found with WBCs ($r = -0.245$, $P = 0.005$), lymphocytes% ($r = -0.586$, $P < 0.001$), RBCs ($r = -0.2488$, $P = 0.005$), Hb (gm/dl) ($r = -0.342$, $P < 0.001$), and HCT ($r = -0.377$, $P < 0.001$). Transferrin and CRP were significantly higher in moderate and severe COVID-19 than mild degree and showed a significant positive correlation with CT score ($r = 0.356$, $P < 0.001$) and ($r = 0.429$, $P < 0.001$), respectively. The most common CT features were peripheral pulmonary GGO and air space consolidation.

Conclusion Clinical features, laboratory assessment, and HRCT imaging had their characteristic signs and performances. Correlating them can make it possible for physicians and radiologists to quickly obtain the final diagnosis and staging of the COVID-19 pneumonia.

Keywords COVID-19 pneumonia · High-resolution CT · Pathophysiological · GGO

✉ Ashraf Anas Zytoon
ashradio@gmail.com

Sameh Mostafa Azab
ashradio2@gmail.com

Zeinab Abdel Aziz Kasemy
ashradio3@gmail.com

Suzan Fouad Omar
ashradio4@gmail.com

Suzy Fayez Ewida
ashradio5@gmail.com

Karim Ayman Sakr
ashradio6@gmail.com

Tarek Fawzy Abd Ella
ashradio7@gmail.com

¹ Radiodiagnosis Department, Faculty of Medicine, Menoufia University, Menoufia, Egypt

² Public Health and Community Medicine Department, Faculty of Medicine, Menoufia University, Menoufia, Egypt

³ Clinical Physiology Department, Faculty of Medicine, Menoufia University, Menoufia, Egypt

⁴ School of Health Sciences, Western University, London, Ontario, Canada

Background

Coronavirus 2 (SARS-CoV-2) is the strain of coronavirus that causes coronavirus disease 2019 (COVID-19), the acute respiratory syndrome responsible for the COVID-19 pandemic [1].

The airway and the vascular bed are the main pathways of pathogenic lung invasion by immunomodulatory viruses inducing lung parenchymal inflammatory/immunologic reactions [2]. The SARS-CoV-2 virus causes viremia by entering the blood through the lungs [3], and then the virus targets the lungs, heart, and renal and gastrointestinal tract as they express angiotensin converting enzyme 2 receptors (ACE2) [4].

Lung involvement by vascular pathway can occur through number of mechanisms including the dysregulated iron homeostasis causing oxidative stress and inflammatory reaction [5] that may promote the sequences of viral infections [6]. Furthermore, anemic hypoxia induces pulmonary vasoconstriction, with an increasing fibrin formation in lung microvasculature [7]; lymphocyte infiltration and sequestration in the lungs [8]. SARS-CoV-2 virus also affects ACE receptor in different tissues including both lymphocyte and lung [4] which leads to marked systemic increase of inflammatory cytokines and mediators that may be even categorized as a “cytokine storm” [9].

Clinical symptoms include fever, fatigue, dry cough, and dyspnea. Most cases had good prognosis [10, 11]. Patients can have severe pneumonia, acute respiratory distress syndrome, and multiple-organ failure, which can lead to death. Mortality rate of 2.1% has been reported [12].

The characteristic chest CT imaging features of COVID-19 pneumonia have low specificity due to their similarity with many other conditions. Though final diagnosis cannot be made based on CT imaging features alone, merging clinical and imaging results can significantly improve the accuracy of diagnosis [13].

CT imaging plays a crucial role in diagnosis and monitoring of disease progress [14–16]. Multiple research studies described the characteristic imaging findings of COVID-19, including ground-glass opacities (GGO) (57 to 88%), bilateral involvement (76 to 88%), and peripheral distribution (33 to 85%) [17–20].

Other imaging features like consolidation, cavitation, and interlobular septal thickening also are reported in some patients. However, these imaging manifestations of COVID-19 are nonspecific and are difficult to differentiate from other pneumonia [21–23].

Therefore, the aim of this study is to learn from the pathophysiological aspects of COVID-19 clinical features, laboratory results, and high-resolution CT manifestations by disease severity to provide important reference values for diagnosis, prevention, and treatment.

Methods

Patients and clinical data

This retrospective analytic study was conducted following the amended Declaration of Helsinki. Our institutional independent ethics committee approved the protocol, and written informed consent was obtained from the patients. This multi-centered study included 128 patients (men 79 and women 49 with mean age \pm SD 49.07 ± 15.89 years; range 13–65 years) from April to July 2020.

In inclusion criteria, we included patients with positive RT-PCR for COVID-19 infection.

In exclusion criteria, we excluded patients with negative RT-PCR for COVID-19 infection as well as patients with a verified additional simultaneous acute illness or other pre-existent medical disorders.

Clinical data were documented, including age, gender, and disease severity. Present history, symptoms and signs, and blood routine outcomes were also recorded. There were three clinical categories according to the severity of disease: “mild, moderate, and severe types.” Patient clinical symptoms ranged between fever, dry cough, muscle ache (myalgia)/fatigue, dyspnea (chest distress), hyposomnia, sore throat (pharyngalgia), and diarrhea (Fig. 1).

Laboratory evaluation

All available laboratory investigations of the patients were analyzed: complete blood count (CBC), hemoglobin and hematocrit level, platelets count, differential white blood cell count, lymphocyte concentration, transferrin level, and level of C reactive protein.



Fig. 1 A 60-year-old male presented with positive RT-PCR and symptoms consistent with COVID-19. Axial unenhanced chest HRCT image shows multifocal, scattered, peripheral, patchy ground-glass opacity in both lungs, and poor definition of area surrounding lesions and associated halo sign at left lung (red arrows)

Radiological evaluation

CT scanning

Each patient underwent chest high-resolution CT (HRCT) examination. Inspiratory phase of chest HRCT examination was achieved during a single-breath hold at full inspiration. The CT scanner models from the hospitals involved in this multi-center study were listed as following: Philips 256-slice Brilliance iCT, Toshiba 16-slice Aquilion, Siemens 16-slice Somatom Emotion. The scanning parameters are as follows: tube voltage 120 kV, tube current 110 mA, pitch 1.0, rotation time ranging from 0.5 to 0.75 s, and slice thickness 5 mm, with 1 mm or 1.5 mm section thickness for axial, coronal, and sagittal reconstructions.

CT assessment

Four radiologists with 15–20 years of experience blinded to clinical data individually scored the CT images.

Basic CT performances

The distribution features and the shape of abnormal attenuation, as well as the involved lung lobes, were documented. If there were any common associated diseases of the lung, such as obsolete pulmonary tuberculosis, emphysema, bronchiectasis, and tumor, they would be recorded if any.

Certain CT signs

The following CT performances features were judged and documented depending upon the following features: ground glass opacification; presence or absence, bilateral or unilateral, site, lobes involved, frequency, pattern “associated consolidation, reverse halo/atoll sign, crazy paving, mosaic attenuation,” morphology, presence of centrilobular nodules or not, presence of tree-in-bud sign or not, presence of solid nodules or not, presence of air space consolidation or not, presence of lymphadenopathy or not and its station, presence of pleural thickening or not, presence of pleural effusion or not, presence of mucoid impaction or not, presence of bronchial wall thickening or not, presence of smooth interlobular septal thickening or not, presence of pulmonary cavitation or not, presence of pericardial effusion or not, and if the patient has endotracheal intubation or not.

Quantified evaluation and CT staging

The CT signs were analyzed quantitatively using a radiologic scoring system, and according to the performances of CT images, the cases were classified into six stages ranging from grade 1 to 2 for mild grades of the disease, 3 to 4 for moderate grades of the disease, and 5 to 6 for severe grades of the

disease, and a total score was eventually recorded. The classification method was mainly according to the previous CT presentations using a CORAD radiologic scoring system of the method previously reported [24].

CORADS 1: COVID-19 is highly unlikely

The CT is normal or there are findings that indicate a non-infectious disease like congestive heart failure, sarcoid, histoplasmosis, malignancy, usual interstitial pneumonia “UIP,” or fibrotic Nonspecific interstitial pneumonia “NSIP.”

CORADS 2: Level of suspicion of COVID-19 infection is low

Findings are consistent with other infections like typical bronchiolitis with tree-in-bud and thickened bronchus walls.

CORADS 3: COVID-19 unsure or indeterminate

CT abnormalities are indication of infection, but unsure whether COVID-19 is involved, like widespread bronchopneumonia, lobar pneumonia, and septic emboli with ground glass opacities.

CORADS 4: The level of suspicion is high.

Mostly these are suspicious CT findings but not extremely typical. Unilateral ground glass, multifocal consolidations without any other typical finding, and findings doubtful of COVID-19 in underlying pulmonary disease are the abovementioned suspicious CT findings which are not extremely typical.

CORADS 5: Multifocal areas of ground glass and consolidation

CORADS 6: *Patient with positive PCR and bilateral GGO (Fig. 2)*

Statistical analysis

Results were statistically evaluated by SPSS version 22 (SPSS Inc., Chicago, IL, USA). ANOVA (F test) was used for parametric data and Kruskal-Wallis tests was used for non-parametric data. Chi-Square (χ^2) and Monte Carlo tests were used for qualitative variables. Spearman correlation was applied. *P* value < 0.05 is considered significant.

Results

Of the features, twenty radiological features and fifteen clinical and laboratory features were nominated to form the

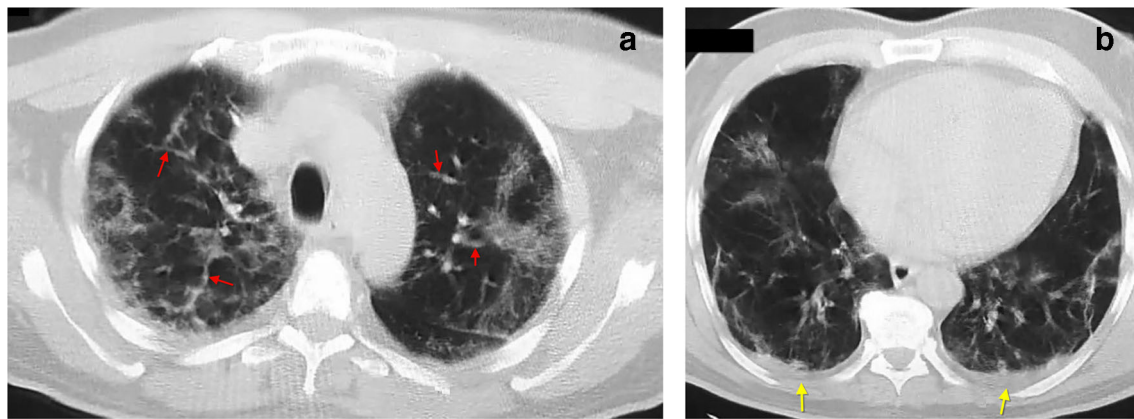


Fig. 2 A 29-year-old female presented with positive RT-PCR and symptoms consistent with COVID-19. A and B, Axial unenhanced chest HRCT images show multifocal, scattered, patchy ground-glass opacity

in both lungs mostly peripheral, and posterior distribution with interlobular septal thickening (red arrows) with reticulation. Minimal bilateral basal pleural effusion (yellow arrows) is seen (B)

predictors based on the results shown in (Table 1). One hundred twenty-eight patients had RT-PCR test findings established to be positive for SARS-CoV-2.

General characteristics and disease grading

Of the 128 patients enrolled in this study cohort with COVID-19 symptoms, 79 (61.7%) were male and 49 (38.3%) were female (mean age \pm SD 49.07 \pm 15.89, range 13–65 years) (Table 1). The mean time interval between symptoms onset and baseline CT was 5 \pm 3 days (range, 2–8 days).

Radiological classification revealed that most of the patients were reported in grade V (55 patients, 43%). COVID severity was distributed as mild grade (19 patients, 14.8%), moderate grade (43 patients, 33.6%), and severe grade (66 patients, 51.6%) (Table 2). Comparison between degrees of severity of COVID-19 regarding demography and pulmonary lesion characteristics revealed that severe COVID-19 symptoms was significantly reported among old age patients ($P = 0.003$) (Fig. 3).

Table 1 General characteristics of the studied patients

Characteristics	No.	%
Age (y) mean \pm SD (range)	49.07 \pm 15.89 (13–65) years	
< 15	4	3.1%
15 < 45	43	33.6%
45 < 65	55	43%
\geq 65	26	20.3%
Sex		
Male	79	61.7%
Female	49	38.3%

Demographic, clinical, pulmonary, and laboratory findings in different disease stages

Patients' age was significantly higher in severe cases (52.89 \pm 13.37). Male to female ratio was nearly equal in mild cases (7.0 to 7.8%) and nearly doubles in severe cases (35.2 to 16.4%) (Table 3).

Clinical symptoms were considerably higher in patients with severe COVID-19 except fever (body temperature 37.5–39.0 $^{\circ}$ C) despite being nonsignificant, but it was higher in patients with moderate COVID-19 in contrast to other groups. Fever (88.3%), cough (76.6%), and muscle ache (myalgia)/fatigue (70.3%) were the most common presenting symptoms (Table 3).

For lab investigations, low lymphocyte and white cell counts were observed in 64.1% and 25% of patients, while high C-reactive protein was observed in 91.4% of patients. Low WBCs was reported among 25% of the whole studied patients. Severe COVID-19 patients revealed a significantly higher percentage of low WBCs (31.8%) than mild COVID-19 (10.5%) and moderate COVID-19 (20.9%) patients. Lymphopenia was

Table 2 Radiological classification of COVID-19

Characteristics	No.	%
Radiological grade		
I	9	7.0%
II	10	7.8%
III	19	14.8%
IV	28	21.9%
V	55	43.0%
VI	7	5.5%
COVID severity		
Mild	19	14.8%
Moderate	43	33.6%
Severe	66	51.6%

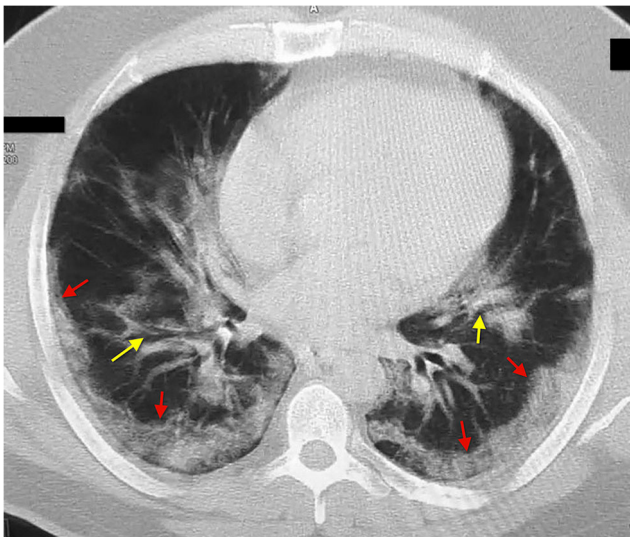


Fig. 3 A 43-year-old female presented with positive RT-PCR and symptoms consistent with COVID-19. Axial unenhanced chest HRCT image demonstrated patchy GGO opacities mixed with consolidation (red arrows) with curvilinear irregular margins under the pleura of both lungs lower lobes with interlobular septal thickening and central air bronchogram (yellow arrows)

significantly reported in 64.1% of all patients, and it was distributed as (0%) for mild COVID-19, (69.8%) for moderate COVID-19, and (78.8%) for severe COVID-19 patients (Fig. 4). Furthermore lymphocytes and WBCs were significantly lower in patients with severe COVID-19 ($P < 0.001$) (Table 4).

RBCs, Hb, and HCT were significantly lower with increasing disease severity (Table 4). High C-reactive protein was detected in 91.4% of patients. Transferrin and CRP were significantly higher in moderate and severe COVID-19 than mild grade ($P = 0.002$ and < 0.001 , respectively) (Table 4).

There is significant positive correlation found between CT score and transferrin ($r = 0.356$, $P < 0.001$) and CRP ($r = 0.429$, $P < 0.001$), and significant negative correlation was found with WBCs ($r = -0.245$, $P = 0.005$), lymphocytes ($r = -0.586$, $P < 0.001$), RBCs ($r = -0.2488$, $P = 0.005$), Hb ($r = -0.342$, $P < 0.001$), and HCT ($r = -0.377$, $P < 0.001$). Weak significant negative correlation was found between CT score and platelets count ($r = -0.176$, $P = 0.047$) (Table 5).

Radiological findings

Pulmonary opacifications were principally sited in the peripheral zone. The sums of involved lung lobes and segments were higher in patients with severe grades than in patients with moderate and mild grades. Bilateral involvement (89.8%) was more predominant than unilateral involvement (10.2%). Lower lobes have higher rates of involvement than the others. The right lower lobe was most often affected (Table 6) (Fig. 5).

The most common CT features were pulmonary GGO in 118 patients, i.e., 92.2% which is distributed as mild 9 patients “7.0%,” moderate 43 patients “33.6%,” and severe 66 patients “51.6%” and air space consolidation in 83 patients, i.e., 64.8% which is distributed as mild 4 patients “3.1%,” moderate 25 patients “19.5%,” and severe 54 patients “42.2%.” Bilateral ground glass opacity and air space consolidation significantly increase with increasing disease severity. Other common findings were bronchial wall thickening in 54 patients, i.e., 42.2% which is distributed as mild 12 patients “9.4%,” moderate 20 patients “15.6%,” and severe 22 patients “17.2%,” and smooth interlobular septal thickening in 82 patients, i.e., 64.1% which is distributed as mild 3 patients “2.3%,” moderate 29 patients “22.7%,” and severe 50 patients “39.1%” (Table 3).

Pleural thickening and effusion were reported in 21 patients (16.4%) and 20 patients (15.6%), respectively. Lymphadenopathy was reported in 39 patients (30.5%). Air space consolidation and pleural effusion were significantly higher among patients with severe COVID-19 than other degrees ($P < 0.0001$ and 0.013, respectively) (Table 6) (Fig. 6).

Discussion

The SARS-CoV-2 infection is well known as a global health hazard. The disease is extremely infectious. It is assumed that infection is transmitted by means of large-particle respiratory droplets produced by coughing or touching contaminated surface [25]. To stop spread of the pandemic, it is critical to detect and make a diagnosis of COVID-19 pneumonia early and to immediately isolate and treat the patient [26]. There are many publications of several studies of COVID-19, which included explanations of the clinical, imaging, and laboratory features of this disease. The current study analysis involved 128 patients with established cases of COVID-19. All clinical features, imaging, and laboratory findings were collected and statistically analyzed as soon as a patient’s diagnosis is confirmed. Particularly, the CT manifestations of COVID-19 disease can provide significant reference values for diagnosis of disease severity which is essential for treatment of patients and can minimize fatality and disease progression in this pandemic situation.

Consistent with outcomes of previous studies [10, 11, 27, 28] as well as ours (61.7% male, and 38.3% female), COVID-19 was more frequently found in men than in women. Furthermore, we found that male/female ratio in mild cases was 9\10 (nearly equal), while in severe cases, it was 45\21 (nearly doubled). In his study, Dai et al., 2020, stated similar results with a greater total number of men (58.1%, 136/234) than that of women (41.9%, 98/234) [29]. A potential description for this finding may be protection provided by the X chromosome and sex hormones, which play an important role

Table 3 Demographics, clinical, pulmonary lesions morphology of patients infected with COVID-19

	Disease severity						χ^2	P value
	Mild (No. = 19, 14.8%)		Moderate (No. = 43, 33.6%)		Severe (No. = 66, 51.6%)			
	No	%	No	%	No	%		
Age (y): mean \pm SD	37.63 \pm 18.10		48.25 \pm 16.23		52.89 \pm 13.37		#11.51	0.003*
Sex:	19	14.8%	43	33.6%	66	51.6%		
Male (No. 79, 61.7%)	9	7.0%	25	19.5%	45	35.2%	3.05	0.217
Female (No. 49, 38.3%)	10	7.8%	18	14.1%	21	16.4%		
Ground glass opacity (No. 118, 92.2%)	9	7.0%	43	33.6%	66	51.6%	62.23	< 0.001* ^{MC}
Side of ground glass opacity	9							
Right (No. 8, 6.2%)	5	3.9%	3	2.3%	0	0.0%	39.90	< 0.001* ^{MC}
Left (No. 3, 2.4%)	0	0.0%	2	1.6%	1	0.8%		
Bilateral (No. 107, 83.6%)	4	3.1%	38	29.7%	65	50.8%		
Air space consolidation (No. 83, 64.8%)	4	3.1%	25	19.5%	54	42.2%	25.17	< 0.001*
Bronchial wall thickening (No. 54, 42.2%)	12	9.4%	20	15.6%	22	17.2%	5.87	0.053
Interlobular septal thickening (No. 82, 64.1%)	3	2.3%	29	22.7%	50	39.1%	23.36	< 0.001*
Interlobular septal thickening Severity	3		19		15		14.18	0.006*
Mild (No. 37, 28.8%)	0	0%	8	6.3%	21	16.5%		
Moderate (No. 29, 22.8%)	0	0%	2	1.6%	14	10.9%		
Severe (No. 16, 12.5%)	0	0%						
Pleural effusion (No. 20, 15.6%)	0	0.0%	4	3.1%	16	12.5%	8.54	0.013* ^{MC}
Symptoms								
Fever (No. 112, 87.5%)	14	11.0%	35	27.3%	63	49.2%	35.9%	0.548
Dry cough (No. 98, 76.6%)	11	8.6%	30	23.5%	57	44.5%	68.84%	< 0.001* ^{MC}
Muscle ache (myalgia) / Fatigue (No. 90, 70.3%)	10	7.8%	25	19.5%	56	43.8%	24.78%	< 0.001*
Dyspnea (chest distress) (No. 76, 59.4%)	2	1.6%	14	10.9%	60	46.9%	60.55%	< 0.001* ^{MC}
Hyposomia (No. 38, 29.7%)	1	0.8%	8	6.3%	29	22.6%	98.35%	< 0.001*
Sore throat (pharyngalgia) (No. 21, 16.5%)	2	1.6%	7	5.5%	12	9.4%	71.10%	< 0.001* ^{MC}
Diarrhea (No. 14, 10.9%)	0	0.0%	3	2.3%	11	8.6%	13.11%	< 0.001* ^{MC}

*Significant #: Kruskal-Wallis

in innate and adaptive immunity [11, 30]. Furthermore, physiologically, female have lower blood indices (e.g., Hb, HCT, and RBCs) than male with lower iron levels. Low iron seems to afford a protective mechanism from infection by restricting iron utilization by the virus [31] and improve the inflammatory condition [32]. Blood indices such as Hb, HCT, RBCs, and transferrin level showed significant changes with increasing disease severity which affects male more than female, suggesting occurrence of dysregulated iron homeostasis alongside the course of COVID-19 disease. It was shown that SARS-CoV-2 protein sequences may form a complex with porphyrin, affecting the 1- β chain of heme of the hemoglobin with subsequent dissociation of the iron [33].

In the current study, Mean \pm SD of Hb content in mild stages of the disease were significantly higher ($P < 0.001$) compared to sever stage (13.37 ± 2.19 vs 11.96 ± 2.45 mg/dl respectively), and the median was 12 in both stages. For HCT% Mean \pm SD in mild stages of the disease were significantly higher ($P < 0.001$) compared to sever stage (40.69 ± 5.22 vs $35.87 \pm 8.71\%$ respectively), and the median were (43 vs 36.5 respectively). There are several reported cases where autoimmune hemolytic anemia occurred during the worsening of symptoms of Covid-19 infection [34–36]. Reduced Hb level with the associated reduction of oxygen carrying capacity of the blood together with CT diagnosed lung parenchymal pathology explains the significant dyspnea associated with increased disease severity.

Fig. 4 Distribution of COVID-19 severity regarding levels of WBCs and lymphocytes

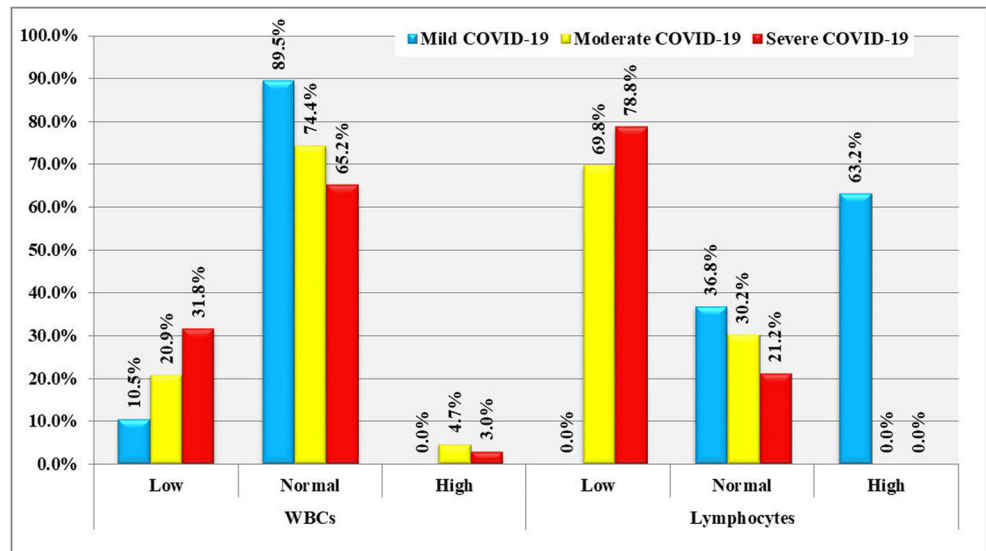


Table 4 Laboratory investigations of patients infected with COVID-19

	Disease severity			Kruskal-Wallis	P value	Post hoc test
	Mild (No. = 19) Mean ± SD	Moderate (No. = 43) Mean ± SD	Severe (No. = 66) Mean ± SD			
WBCs *10 ³	8.64 ± 2.90	5.48 ± 2.05	5.02 ± 1.68	10.25	0.006*	P ₁ = 0.023*
• Median	7.0	5.50	5.50			P ₂ = 0.001*
• IQR	5.10–7.90	3.50–7.0	3.0–6.60			P ₃ = 0.373
Lymphocytes %	40.60 ± 5.91	19.98 ± 6.34	16.0 ± 4.76	54.45	< 0.001*	P _{1,2} < 0.001
• Median	42	19	17			P ₃ = 0.002*
• IQR	36–45.5	15–26	13–19			
RBCs *10 ⁶	4.96 ± 0.65	5.63 ± 2.56	5.31 ± 2.62	8.24	0.016*	P ₁ = 0.417
• Median	5	5	4.80			P ₂ = 0.098
• IQR	4.7–5.5	4.7–5.3	4.5–5			P ₃ = 0.005*
Hb (gm/dl)	13.37 ± 2.19	13.83 ± 0.94	11.96 ± 2.45	F = 11.84	< 0.001*	P ₁ = 0.447
• Median	12	14	12			P ₂ = 0.016*
• IQR	11.9–16	12.8–14.7	11–14			P ₁ < 0.001*
HCT %	40.69 ± 5.22	41.39 ± 4.54	34.87 ± 8.71	F = 12.65	< 0.001*	P ₁ = 0.643
• Median	43	43	36.5			P ₂ = 0.003*
• IQR	34–45	40–44	29.75–42			P ₁ < 0.001*
Platelets *10 ³	213.63 ± 36.17	187.97 ± 63.77	169.95 ± 72.59	4.11	0.128	P ₁ = 0.390
• Median	215	227	172.50			P ₂ = 0.042*
• IQR	215–252	162–230	162–227			P ₁ = 0.276
Transferrin ng/mL	123.36 ± 23.98	386.90 ± 250.33	478.60 ± 381.73	11.99	< 0.001*	P _{1,2} < 0.001*
• Median	103	257.50	261			P ₁ = 0.389
• IQR	103–150	175–645	175–905.75			
CRP (mg/L)	28.38 ± 11.13	123.15 ± 110.11	154.23 ± 129.96	26.86	< 0.001*	P ₁ = 0.067
• Median	23	100	87			P ₁ < 0.001*
• IQR	23–44	23–87	69–245			P ₁ = 0.094

*Significant P1: mild vs. Moderate, P2: Mild vs. severe, P3: Moderate vs. severe, IQR: Interquartile range

Table 5 Correlation between CT score and lab investigations

	CT score		
	r_s	<i>P</i> value	CI 95%
WBCs*10 ³	−0.245	0.005*	(−0.42)–(−0.05)
Lymphocytes%	−0.586	<0.001*	(−0.71)–(−0.43)
RBCs*10 ⁶	−0.248	0.005*	(−0.40)–(−0.06)
Hb(gm/dl)	−0.342	<0.001*	(−0.51)–(−0.16)
HCT%	−0.377	<0.001*	(−0.52)–(−0.20)
Platelets*10 ³	−0.176	0.047*	(−0.33)–(−0.01)
Transferrin	0.356	<0.001*	0.20-0.50
CRP(mg/L)	0.429	<0.001*	0.27-0.56

*significant

The COVID-19 disease severity significantly increased with old age and was milder in younger age which was in concordance with several other studies [37–39]. This can be explained by poor health outcomes and the physiologic changes of aging which begin early in life with the drop in production of new T cells due to thymus gland involution, followed by deterioration of the immune system and increased susceptibility to infection [40]. Seventy to eighty percent of the circulating lymphocytes are composed of T lymphocytes [41].

In his study, Han et al. 2020 stated that the wide-ranging initial clinical symptoms which are fever, dry cough, and fatigue were common. Ninety-four of 108 (87%) patients had fever (range, 37.3–38.5 °C), which was followed in frequency by dry cough (60%) and fatigue (39%) [26]. Furthermore Dai et al., 2020, reach to similar results in his study with fever and cough as the chief symptoms. However, some patients presented primarily with atypical symptoms, such as diarrhea, nausea, and vomiting [29]. Similar to the previous results, the patients enrolled in the current study presented with fever (88.3%, range, 37.5–40 °C), cough (76.6%), and muscle ache (myalgia)/fatigue (70.3%) as the most common presenting symptoms, while diarrhea represent 10.9% (Fig. 7).

In the current study, laboratory results displayed the characteristics of viral infection in most of our patients, such as normal (71.9%) or decreased (25%) WBCs count (patients with normal and decreased WBCs count represent 96.9%) and decreased lymphocyte count (64.1%) and elevated high-sensitivity C-reactive protein CRP level (91.2%) due to inflammation. Our results are in line parallel with previous studies; in his study, Han et al.'s laboratory results showed normal or reduced WBC count (100%), reduced lymphocyte count (60%), and elevated CRP (99%) [26].

Seventy to eighty percent of the circulating lymphocytes are composed of T lymphocytes [41], which explain the significant lymphopenia frequently noted in COVID-19 [42–44] and was associated with poor outcome and increases degree of severity in patients with COVID-19. In addition, in sever COVID-19

infection peripheral T lymphocytes are further reduced due to lymphocyte sequestration in specific target organs [8], lymphocyte affection through ACE2 receptor, which may be a direct target of SARS-CoV-2 infection [45], and lymphocyte affection by pro-inflammatory cytokines production especially IL-6 [3].

In the present study, lymphopenia was significantly reported in 64.1% of all patients, and it was distributed as 0% for mild COVID-19, 69.8% for moderate COVID-19, and 78.8% for severe COVID-19 patients. For lab investigations, lymphocytes and Hb were significantly lower in patients with severe COVID-19 ($P < 0.001$).

High-resolution CT can depict millimeter-size lesions and play an important role in early diagnosis of COVID-19 pneumonia [17, 46, 47]. In a study of 41 patients, Huang et al., 2020, stated that 40 patients (98%) had bilateral while 1 (2%) had unilateral involvement. They stated that the characteristic chest CT signs for patients with severe symptoms admitted to the ICU were bilateral, multiple, lobular, and subsegmental areas of consolidation, whereas findings for patients with mild symptoms not admitted to the ICU were bilateral GGO and subsegmental areas of consolidation [10]. In a study of 99 patients, Chen et al., 2020, stated that 74 patients (75%) had bilateral pneumonia, with just 25 (25%) having unilateral pneumonia [11]. In a study of 51 patients, Song et al., 2020, reported that pure GGOs were detected in 77% of patients and that they showed principally bilateral, posterior, and peripheral distribution [18]. Such data are related to our results with 83.6% of our patients having bilateral distribution and 8.6% having unilateral distribution with slight difference between our results and the previous literature that could be explained by the difference in patient population number included in each cohort study. The typical CT manifestations of COVID-19 were in concordance with Wang et al., 2020, and Kanne et al., 2020, which are bilateral, basal, and peripheral ground glass opacities (GGOs), i.e., 92.2% and consolidation in nearly 58.6% of patients [44, 48]. Although consolidation associated with round opacities and septal thickening are more common in COVID-19 according to Parekh et al. 2020 [13], our finding revealed GGO with higher non-round opacities (74.2%), which can be useful in differentiating COVID-19 pneumonia from other patterns of lung pathology (Fig. 8).

Chen et al., 2020, reported 14 patients (14%) had many areas of mottling and GGO, while Lei et al., 2020, reported a patient with numerous peripheral GGO in both lungs [11, 20]. In a study by Chan et al., 2020, six of seven patients had multifocal patchy GGO on CT, principally around the peripheral parts of the lungs [49]. Overall, according to Bai et al. 2020, compared to non-COVID-19 viral pneumonia, parenchymal opacities in COVID-19 pneumonia were more likely to be peripheral (80% vs. 57%), and have GGO (91% vs. 68%). COVID-19 patients were less probably to have central and peripheral distribution (14% vs. 35%) [13, 24]. In the present study, 63.3% of our patients have diffuse GGO opacities while 27.3% have peripheral and 1.6% have central distribution.

Table 6 Radiological characteristics of the studied patients

Characteristics	No.	%
Ground glass opacity		
Positive	118	92.2%
Negative	10	7.8%
Side of ground glass opacity (<i>n</i> = 118)		
Bilateral	107	83.6%
Right	8	6.3%
Left	3	2.3%
Site of Ground glass opacity (<i>n</i> = 118)		
Diffuse	81	63.3%
Peripheral	35	27.3%
Central	2	1.6%
Distribution of ground glass opacity (<i>n</i> = 118)		
Upper + middle + lower	70	54.7%
Middle + lower	19	14.8%
Lower	18	14.1%
Upper + lower	6	4.7%
Upper + middle	3	2.3%
Upper	2	1.6%
Frequency of ground glass opacity (<i>n</i> = 118)		
Multiple	112	87.5%
Single	6	4.7%
Pattern of ground glass opacity (<i>n</i> = 118)		
Mosaic attenuation + consolidation + reverse halo/atoll sign	48	37.5%
Mosaic attenuation + reverse halo/atoll sign	33	25.8%
Crazy paving + consolidation + reverse halo/atoll sign	22	17.2%
Reverse halo/atoll sign	6	4.7%
Consolidation + reverse halo/atoll sign	5	3.9%
Crazy paving + reverse halo/atoll sign	4	3.1%
Morphology pattern (<i>n</i> = 118)		
Not rounded	95	74.2%
Rounded	33	25.8%
Centrilobular nodules/tree-in-bud sign		
Positive	39	30.5%
Negative	89	69.5%
Solid nodule(s)		
Positive	38	29.7%
Negative	90	70.3%
Air space consolidation		
Positive	83	64.8%
Negative	45	35.2%
Lymphadenopathy		
Positive	39	30.5%
Negative	89	69.5%
Site of Lymphadenopathy (<i>n</i> = 39)		
Mediastinal	39	100.0%
Pleural thickening		
Positive	21	16.4%
Negative	107	83.6%
Pleural effusion		

Table 6 (continued)

Characteristics	No.	%
Positive	20	15.6%
Negative	108	84.4%
Mucoid impaction		
Positive	26	20.3%
Negative	102	79.7%
Bronchial wall thickening		
Positive	54	42.2%
Negative	74	57.8%
Smooth interlobular septal thickening		
Positive	82	64.1%
Negative	46	35.9%
Smooth interlobular septal thickening ($n = 82$)		
Mild	37	28.9%
Moderate	29	22.7%
Severe	16	12.5%
Pulmonary cavities		
Positive	3	2.3%
Negative	125	97.7%
Endotracheal intubation		
Positive	5	3.9%
Negative	123	96.1%
Pericardial effusion		
Positive	2	1.6
Negative	126	98.4

*Significant

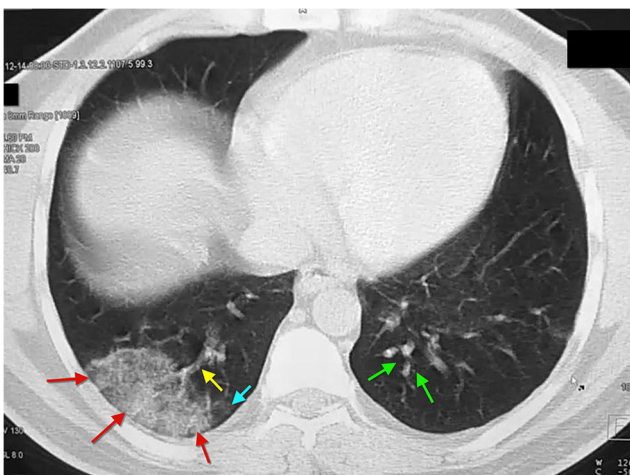


Fig. 5 A 28-year-old male presented with positive RT-PCR and symptoms consistent with COVID-19. Axial unenhanced chest HRCT image shows right lower lobe peripheral patchy GGO (red arrows), tree-in-bud sign (green arrows), and vascular thickening (yellow arrow) with poor definition of the area surrounding lesion (blue arrow)

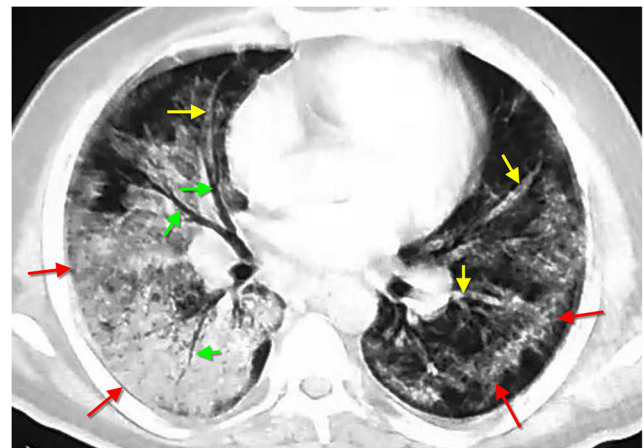


Fig. 6 A 59-year-old female presented with positive RT-PCR and symptoms consistent with COVID-19. a. Axial unenhanced chest HRCT image demonstrated diffuse right lower lobar consolidation opacification with left lung lower lobar large GGO mixed with consolidation with bilateral crazy paving pattern (red arrows), air bronchogram (green arrows), halo sign, vascular thickening, and interlobular septal thickening (yellow arrows), with poor definition of the other areas surrounding lesions

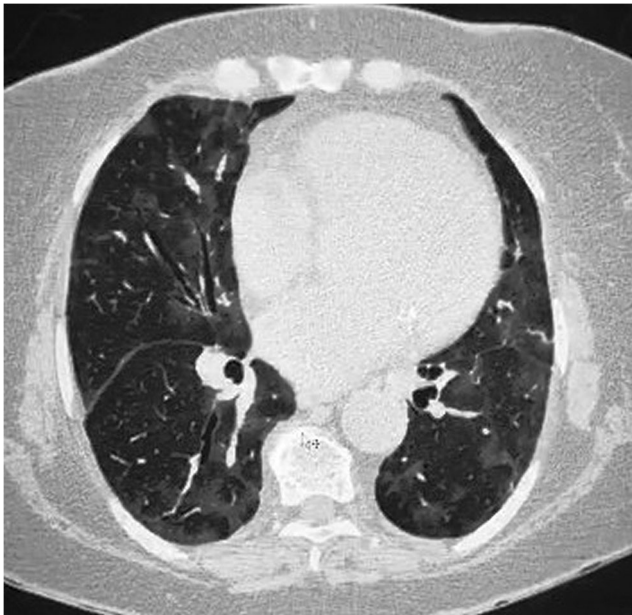


Fig. 7 A 72-year-old female presented with positive RT-PCR and symptoms consistent with COVID-19. Axial unenhanced chest HRCT image shows bilateral lower lobar peripheral and central multiple patchy GGO with crazy paving pattern, air bronchogram, halo sign, vascular thickening, and interlobular septal thickening with poor definition of the other areas surrounding lesions

Cheng et al., 2020, in his study, found mixed GGO and consolidation in patients with positive RT-PCR test results, the most frequently detected opacification in patients with COVID-19 was GGO (100.0% [11/11]), which appeared

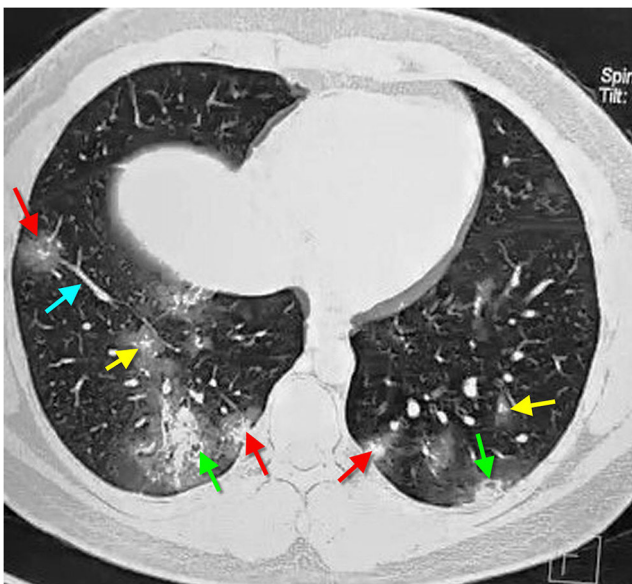


Fig. 8 A 49-year-old male presented with positive RT-PCR and symptoms consistent with COVID-19. Axial unenhanced chest HRCT image demonstrated bilateral basal peripherally located under the pleura GGO mixed with consolidation (red arrows), of ill-defined boundary, air bubble sign (green arrows), halo sign (yellow arrows), and air bronchogram, vascular thickening, and interlobular septal thickening (blue arrows)

mainly in the peripheral zone and most often involved lower lung lobes and segments. This strongly suggests that GGO is the most common imaging manifestation among patients with COVID-19, which is useful in diagnosing and isolating cases while they are in the early stage of the disease. It is worth mentioning that the appearance of the GGO was round or oval rather than patchy [10]. Equivalent to previous studies, GGO patterns were found in 92.2% of our patients.

Comparable with the outcome of a former study by Chan et al., 2020, pleural effusion and lymphadenopathy were not detected. In our study, pleural effusion (15.6%) and lymphadenopathy (30.5%) were found which could be explained by the limited number (five patients) of population in Chan et al.'s study [49] (Fig. 9).

In the current study, CT findings of GGO found that lesions were found in 92.2% of our patients, 90.6% have peripheral distribution, and 88.3% were located in the lower lobes. The lesions involved one lobe in 15.6% and two or more lobes in 76.6% of the patients. In the current study, the lower lobe was the most affected part (14.1%) in single lobar affection. This was in agreement with Han et al. (2020) who stated that in primary CT findings, when the lesions involved two or more lobes, it were essentially distributed in the peripheral zones of the lung, while in single lobe involvement, it was usually in the right lower lobe [26]. This finding may be related to the anatomy of the right lower lobe bronchus, which is thick and short, making it easy for the virus to attack it. Regarding the diffuse radiological characteristics of the studied patients with more tendency to basal lung affection and the correlation between lung CT score and lab investigations (WBCs, lymphocytes%, RBCs, Hb, HCT, platelets, transferrin, and CRP), these results suggest additional blood involvement in COVID-19 lung pathophysiology.

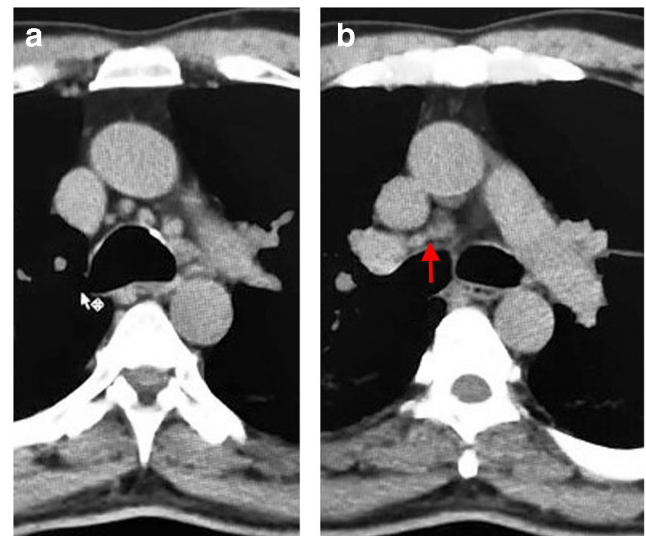


Fig. 9 A 49-year-old male presented with positive RT-PCR and symptoms consistent with COVID-19. Axial unenhanced chest HRCT image demonstrated mediastinal lymphadenopathy (red arrows)

Furthermore, Han et al., 2020, found that COVID-19 pneumonia is common in adults (mean age, 45 years) but infrequent in children and infants [26]. In his study, Cheng et al., 2020, the youngest patient in the present study is a 25-year-old male [28]. In the current study, the mean age \pm SD is 49.07 ± 15.89 , range 13–65 years. The youngest patient is a 13-year-old-male and the oldest is a 85-year-old male. Our patients' age categories were 3.1% (< 15 years), 33.6% (15 < 45 years), 43% (45 < 65 years), and 20.3% (\geq 65 years).

COVID-19 demonstrations are more widespread GGO than consolidation, which is in harmony with clinical findings [50–55]. There is a wide-ranging CT signs of viral pneumonia. Even though not all cases of viral pneumonia have the classic imaging patterns, most cases have similar manifestations on imaging and are related to the pathogenesis of pulmonary viral infection [56].

Han et al., 2020, found that fairly characteristic manifestations were halo sign (64%), crazy paving pattern (40%), and air bronchogram sign (48%) [26]. Why are GGO and the halo sign early CT manifestations? The pathophysiologic mechanism is not clear. It may that inflammatory cytokine storm causes pneumonia with early pathologic finding diffuse alveolar damage. Since the hyaline membrane is between the alveolar walls, exudation and edema in the alveoli are not obvious, perhaps initiating GGO on CT images [10].

Dai et al., 2020, stated in his study the characteristic signs on CT images. The atypical attenuations were highly commonly located in bilateral multiple lung lobes and disseminated in the lower and/or periphery of the lungs with frequent signs, for example, interlobular septal thickening, air bronchus sign, pleural thickening, solid nodules, and reticular/mosaic sign. Additionally, a few cases of mediastinal lymphadenopathy, pleural effusion, and pericardial effusion were detected [29]. According to Bai et al. 2020, in contrast to non-COVID-19 viral pneumonia, parenchymal opacities in COVID-19 pneumonia state that COVID-19 patients were less likely to have air bronchograms (14% vs. 23%), pleural thickening (15% vs. 33%), pleural effusion (4 vs. 39%), and lymphadenopathy (2.7% vs. 10.2%) [13, 24].

Reversed halo sign and pulmonary nodules associated with COVID-19 have not been formerly described with severe acute respiratory syndrome (SARS) and Middle East respiratory syndrome (MERS). Lung abnormalities in SARS are more frequently described to be unifocal [57]. Our study agree with those distinguishing CT manifestations; 83.6% of our patients have ground glass opacities GGOs which were the most frequently seen in each CT stages with different CT manifestations; reverse halo/atoll sign (92.2%), mosaic attenuation (63.3%), consolidation (58.6%), bronchial wall thickening (42.2%), and crazy paving (20.3%). GGO assumes rounded shape in (25.8%). In addition to the characteristic GGO, another CT manifestation was also recorded; centrilobular nodules/tree-in-bud sign 30.5%, solid nodule(s)

29.7%, bronchial wall thickening 42.2%, interlobular septal thickening 64.1%, and mucoid impaction 20.3%. The frequency of pulmonary cavities 2.3%, pleural thickening 16.4%, pleural effusion 15.6%, mediastinal lymphadenopathy (30.5%), and pericardial effusion (1.6%) was relatively small. These CT performances of COVID-19 were in line parallel to the earlier studies [17, 26, 28, 29]. Our results suggested that each clinical, laboratory and imaging (especially CT) finding had their characteristic signs and performances, making it feasible for physicians and radiologists to quickly make the final diagnosis and staging of the COVID-19 pneumonia.

There were limitations to this study that should be declared. First, the number of study cohort is small; a larger cohort study would be useful to further explore the details of imaging findings. Further research with use of a more sample size is necessary to explore the applicability of the clinical, laboratory, and radiological findings in predicting the prognosis of COVID-19, so further studies that include long-term follow-up CT examinations are needed to investigate the entire course of the disease and to evaluate disease progression/regression after treatment efficacy. Second, lung tissue biopsies or even autopsy to investigate the relation between CT findings and histopathologic appearances were not available. Third, the patients performed the CT scans with different machine type, due to the multiple centers in the study. The heterogeneity of the CT data might influence the results of the study. As a final point, this was a retrospective study. A further longitudinal research was needed to provide dynamic CT assessment for pulmonary lesions and to obtain the data of long term pulmonary function changes.

Conclusion

In conclusion, the commonest clinical characteristics of COVID-19 pneumonia were fever, cough, and muscle ache (myalgia)/fatigue, while the most frequent laboratory abnormalities encountered were low lymphocyte and WBCs and high CRP. Review of chest CT shows that bilateral pulmonary GGO and air space consolidation predominantly located in the peripheral zones mainly the right lower lobe were the typical radiological findings with more lobes involvement indicate aggravation of the disease. This study highlighted the importance of HRCT imaging features combined with clinical and laboratory assessment for accurate and quick diagnosis and staging of COVID-19 pneumonia patients.

Authors' contributions All authors have read and approved the manuscript.

Sameh Mostafa Azab.

1. Substantial contribution to the conception of the study.

2. Substantial contribution to the design of the study.
 3. Substantial contribution to the acquisition, analysis of the data.
 4. Substantial contribution to the interpretation of data.
 5. Substantial contribution to the creation of the final work.
 6. Substantial contribution to the study revision.
 7. Substantial contribution to the accuracy or integrity of the submitted manuscript.

Ashraf Anas Zytoon.

1. Substantial contribution to the conception of the study.
 2. Substantial contribution to the design of the study.
 3. Substantial contribution to the acquisition, analysis of the data.
 4. Substantial contribution to the interpretation of data.
 5. Substantial contribution to the creation of the final work.
 6. Substantial contribution to the study revision.
 7. Substantial contribution to the accuracy or integrity of the submitted manuscript.

Zeinab Abdel Aziz Kasemy

1. Substantial contribution to the conception of the study.
 2. Substantial contribution to the design of the study.
 3. Substantial contribution to the acquisition, analysis of the data.
 4. Substantial contribution to the interpretation of data.
 5. Substantial contribution to the creation of the final work.
 6. Substantial contribution to the study revision.
 7. Substantial contribution to the accuracy or integrity of the submitted manuscript.

Suzan Fouad Omar

1. Substantial contribution to the conception of the study.
 2. Substantial contribution to the design of the study.
 3. Substantial contribution to the acquisition, analysis of the data.
 4. Substantial contribution to the interpretation of data.
 5. Substantial contribution to the creation of the final work.
 6. Substantial contribution to the study revision.
 7. Substantial contribution to the accuracy or integrity of the submitted manuscript.

Suzy Fayeze Ewida

1. Substantial contribution to the conception of the study.
 2. Substantial contribution to the design of the study.
 3. Substantial contribution to the acquisition, analysis of the data.
 4. Substantial contribution to the interpretation of data.
 5. Substantial contribution to the creation of the final work.
 6. Substantial contribution to the study revision.
 7. Substantial contribution to the accuracy or integrity of the submitted manuscript.

Karim Ayman Abdelrahman Sakr

1. Substantial contribution to the idea of the study.
 2. Substantial contribution to the analysis of the data.
 3. Substantial contribution to the study english revision.
 Tarek Fawzy Abd Ella
 1. Substantial contribution to the conception of the study.
 2. Substantial contribution to the design of the study.
 3. Substantial contribution to the acquisition, analysis of the data.
 4. Substantial contribution to the interpretation of data.
 5. Substantial contribution to the creation of the final work.
 6. Substantial contribution to the study revision.
 7. Substantial contribution to the accuracy or integrity of the submitted manuscript.

Data availability The datasets generated or analyzed during current study are not publicly available due to patients' individual privacy.

Compliance with ethical standards

Ethics approval and consent to participate Our study was approved by ethical and scientific committee - Faculty of Medicine - Menoufia University Ref. No. 5/2020/RAD 8.

Consent to participate Written informed consent form was obtained from every patient after detailed explanation of the study.

Consent for publication All authors gave consent to publish the study data.

Competing interests The authors declare that they have no conflict of interest.

Abbreviations CT, computed tomography; HRCT, high-resolution computed tomography; RBCs, red blood cells; Hb, hemoglobin concentration; HCT, hematocrit; CRP, C-reactive protein test; SARS, severe acute respiratory syndrome; SARS-CoV-2, severe acute respiratory syndrome coronavirus 2; RT-PCR, reverse transcription polymerase chain reaction; CBC, complete blood count; UIP, usual interstitial pneumonia; NSIP, fibrotic Nonspecific interstitial pneumonia; GGO, ground-glass opacification/opacity; WBCs, white blood cells; ACE2, angiotensin-converting enzyme 2; SARS, severe acute respiratory syndrome

References

- Gorbalenya AE, Baker SC, Baric RS et al (2020) The species severe acute respiratory syndrome-related coronavirus: classifying 2019-nCoV and naming it SARS-CoV-2. *Nat Microbiol* 5:536–544. <https://doi.org/10.1038/s41564-020-0695-z>
- Poletti V, Costabel U, Semenzato G (2005) Pulmonary complications in patients with hematological disorders: pathobiological bases and practical approach. *Semin Respir Crit Care Med* 26:439–444. <https://doi.org/10.1055/s-2005-922028>
- Lin L, Lu L, Cao W, Li T (2020) Hypothesis for potential pathogenesis of SARS-CoV-2 infection—a review of immune changes in patients with viral pneumonia. *Emerg Microbes Infect* 9:727–732. <https://doi.org/10.1080/22221751.2020.1746199>
- Ni W, Yang X, Yang D et al (2020) Role of angiotensin-converting enzyme 2 (ACE2) in COVID-19. *Crit Care* 24:422. <https://doi.org/10.1186/s13054-020-03120-0>
- Dalamaga M, Karampela I, Mantzoros CS (2020) Commentary: could iron chelators prove to be useful as an adjunct to COVID-19 treatment regimens? *Metabolism*. 108:154260. <https://doi.org/10.1016/j.metabol.2020.154260>
- Drakesmith H, Prentice A (2008) Viral infection and iron metabolism. *Nat Rev Microbiol* 6:541–552. <https://doi.org/10.1038/nrmicro1930>
- Cavezzi A, Troiani E, Corrao S (2020) COVID-19: hemoglobin, iron, and hypoxia beyond inflammation. A narrative review. *Clin Pract* 10:1271. <https://doi.org/10.4081/cp.2020.1271>
- Li T, Qiu Z, Zhang L et al (2004) Significant changes of peripheral T lymphocyte subsets in patients with severe acute respiratory syndrome. *J Infect Dis* 189:648–651. <https://doi.org/10.1086/381535>
- Gabriella DM, Cristina S, Concetta R, Francesco R, Annalisa C (2020) SARS-Cov-2 infection: response of human immune system and possible implications for the rapid test and treatment. *Int Immunopharmacol* 84:106519. <https://doi.org/10.1016/j.intimp.2020.106519>
- Huang C, Wang Y, Li X et al (2020) Clinical features of patients infected with 2019 novel coronavirus in Wuhan, China. *Lancet* 395:497–506. [https://doi.org/10.1016/S0140-6736\(20\)30183-5](https://doi.org/10.1016/S0140-6736(20)30183-5)
- Chen N, Zhou M, Dong X et al (2020) Epidemiological and clinical characteristics of 99 cases of 2019 novel coronavirus pneumonia in Wuhan, China: a descriptive study. *Lancet* 395:507–513. [https://doi.org/10.1016/S0140-6736\(20\)30211-7](https://doi.org/10.1016/S0140-6736(20)30211-7)
- Patel A, Jernigan D (2020) 2019-nCoV CDC Response Team. Initial public health response and interim clinical guidance for the

- 2019 novel coronavirus outbreak - United States, December 31, 2019-February 4, 2020. *Am J Transplant* 20:889–895. <https://doi.org/10.1111/ajt.15805>
13. Parekh M, Donuru A, Balasubramanya R, Kapur S (2020) Review of the chest CT differential diagnosis of ground-glass opacities in the COVID era. *Radiology* 202504. <https://doi.org/10.1148/radiol.2020202504>
 14. Pan Y, Guan H (2020) Imaging changes in patients with 2019-nCoV. *Eur Radiol* 30:3612–3613. <https://doi.org/10.1007/s00330-020-06713-z>
 15. Pan Y, Guan H, Zhou S et al (2020) Initial CT findings and temporal changes in patients with the novel coronavirus pneumonia (2019-nCoV): a study of 63 patients in Wuhan, China. *Eur Radiol* 30:3306–3309. <https://doi.org/10.1007/s00330-020-06731-x>
 16. Kim H (2020) Outbreak of novel coronavirus (COVID-19): what is the role of radiologists? *Eur Radiol* 30:3266–3267. <https://doi.org/10.1007/s00330-020-06748-2>
 17. Chung M, Bernheim A, Mei X et al (2020) CT imaging features of 2019 novel coronavirus (2019-nCoV). *Radiology* 295:202–207. <https://doi.org/10.1148/radiol.2020200230>
 18. Song F, Shi N, Shan F et al (2020) Emerging coronavirus 2019-nCoV pneumonia. *Radiology* 295:210–217. <https://doi.org/10.1148/radiol.2020200274>
 19. Kanne JP (2020) Chest CT findings in 2019 novel coronavirus (2019-nCoV) infections from Wuhan, China: key points for the radiologist. *Radiology* 295:16–17. <https://doi.org/10.1148/radiol.2020200241>
 20. Lei J, Li J, Li X (2020) Qi X (2020) CT imaging of the 2019 novel coronavirus (2019-nCoV) pneumonia. *Radiology* 295:18. <https://doi.org/10.1148/radiol.2020200236>
 21. Ng M-Y, Lee EY, Yang J et al (2020) Imaging profile of the COVID-19 infection: radiologic findings and literature review. *Radiology:Cardiothoracic Imaging*:2. <https://doi.org/10.1148/ryct.2020200034>
 22. Kay F, Abbara S (2020) The many faces of COVID-19: spectrum of imaging manifestations. *Radiology:Cardiothoracic Imaging* 2. <https://doi.org/10.1148/ryct.2020200037>
 23. Wu Y, Xie Y, Wang X (2020) Longitudinal CT findings in COVID-19 pneumonia: case presenting organizing pneumonia pattern. *Radiology:Cardiothoracic Imaging* 2020:2. <https://doi.org/10.1148/ryct.2020200031>
 24. Bai HX, Hsieh B, Xiong Z et al (2020) Performance of radiologists in differentiating COVID-19 from non-COVID-19 viral pneumonia at chest CT. *Radiology* 296:E46–E54. <https://doi.org/10.1148/radiol.2020200823>
 25. Swerdlow DL, Finelli L (2020) Preparation for possible sustained transmission of 2019 novel coronavirus: lessons from previous epidemics. *JAMA* 323:1129–1130. <https://doi.org/10.1001/jama.2020.1960>
 26. Han R, Huang L, Jiang H, Dong J, Peng H, Zhang D (2020) Early clinical and CT manifestations of coronavirus disease 2019 (COVID-19) pneumonia. *Am J Roentgenol* 215:338–343. <https://doi.org/10.2214/AJRAMJROENTGENOL.20.22961>
 27. Li Q, Guan X, Wu P et al (2020) Early transmission dynamics in Wuhan, China, of novel corona virus infected pneumonia. *N Engl J Med* 382:1199–1207
 28. Cheng Z, Lu Y, Cao Q et al (2020) Clinical features and chest CT manifestations of coronavirus disease 2019 (COVID-19) in a single-center study in Shanghai, China. *Am J Roentgenol* 215:121–126. <https://doi.org/10.2214/AJRAMJROENTGENOL.20.22959>
 29. Dai H, Zhang X, Xia J et al (2020) High-resolution chest CT features and clinical characteristics of patients infected with COVID-19 in Jiangsu, China. *Int J Infect Dis* 95:106–112. <https://doi.org/10.1016/j.ijid.2020.04.003>
 30. Jaillon S, Berthenet K, Garlanda C (2019) Sexual dimorphism in innate immunity. *Clin Rev Allergy Immunol* 56:308–321. <https://doi.org/10.1007/s12016-017-8648-x>
 31. Moalem S, Weinberg ED, Percy ME (2004) Hemochromatosis and the enigma of misplaced iron: implications for infectious disease and survival. *Biometals*. 17:135–139. <https://doi.org/10.1023/b:biom.0000018375.20026.b3>
 32. Resnick MW (2010) Iron homeostasis and the inflammatory response. *Annu Rev Nutr* 30:105–122. <https://doi.org/10.1146/annurev.nutr.012809.104804>
 33. Liu W, Li H COVID-19: Attacks the 1-beta chain of hemoglobin and captures the porphyrin to inhibit human heme metabolism. *ChemRxiv*. <https://doi.org/10.26434/chemrxiv.11938173.v9>
 34. Lopez C, Kim J, Pandey A, Huang T, DeLoughery TG (2020) Simultaneous onset of COVID-19 and autoimmune haemolytic anaemia. *Br J Haematol* 190:31–32. <https://doi.org/10.1111/bjh.16786>
 35. Hindilerden F, Yonal-Hindilerden I, Akar E, Yesilbag Z, Kart-Yasar K (2020) Severe autoimmune hemolytic anemia in COVID-19 infection, safely treated with steroids. *Mediterr J Hematol Infect Dis* 12:e2020053. <https://doi.org/10.4084/MJHID.2020.053>
 36. Lazarian G, Quinquenel A, Bellal M et al (2020) Autoimmune hemolytic anemia associated with COVID-19 infection. *Br J Haematol* 190:29–31. <https://doi.org/10.1111/bjh.16794>
 37. Nikolich-Zugich J, Knox KS, Rios CT, Natt B, Bhattacharya D, Fain MJ (2020) SARS-CoV-2 and COVID-19 in older adults: what we may expect regarding pathogenesis, immune responses, and outcomes. *Geroscience* 42:505–514. <https://doi.org/10.1007/s11357-020-00186-0>
 38. Wang D, Hu B, Hu C et al (2020) Clinical characteristics of 138 hospitalized patients with 2019 novel coronavirus-infected pneumonia in Wuhan, China. *JAMA* 323:1061–1069. <https://doi.org/10.1001/jama.2020.1585>
 39. Parri N, Lenge M, Buonsenso D (2020) Coronavirus infection in pediatric emergency departments (CONFIDENCE) research group. Children with Covid-19 in Pediatric Emergency Departments in Italy. *N Engl J Med* 383:187–190. <https://doi.org/10.1056/NEJMc2007617>
 40. Haroun HSW (2018) Aging of thymus gland and immune system. *MOJ Anat & Physiol* 5:178–181. <https://doi.org/10.15406/mojap.2018.05.00186>
 41. Greer JP, Arber DA, Glader DE, List AF, Robert T, Means RT Jr, Rodgers GM (2018) Wintrobe's clinical hematology. Volume 2, 12th edn. Lippincott Williams & Wilkins, Philadelphia
 42. Yang X, Yu Y, Xu J et al (2020) Clinical course and outcomes of critically ill patients with SARS-CoV-2 pneumonia in Wuhan, China: a single-centered, retrospective, observational study. *Lancet Respir Med* 8:475–481. [https://doi.org/10.1016/S2213-2600\(20\)30079-5](https://doi.org/10.1016/S2213-2600(20)30079-5)
 43. Ruan Q, Yang K, Wang W, Jiang L, Song J (2020) Clinical predictors of mortality due to COVID-19 based on an analysis of data of 150 patients from Wuhan, China. *Intensive Care Med* 46:846–848. <https://doi.org/10.1007/s00134-020-05991-x>
 44. Wang Y, Dong C, Hu Y et al (2020) Temporal changes of CT findings in 90 patients with COVID-19 pneumonia: a longitudinal study. *Radiology* 296:E55–E64. <https://doi.org/10.1148/radiol.2020200843>
 45. Xu H, Zhong L, Deng J et al (2020) High expression of ACE2 receptor of 2019-nCoV on the epithelial cells of oral mucosa. *Int J Oral Sci* 12:1–5. <https://doi.org/10.1038/s41368-020-0074-x>
 46. Paul NS, Roberts H, Butany J et al (2004) Radiologic pattern of disease in patients with severe acute respiratory syndrome: the Toronto experience. *Radiographics* 24:553–563. <https://doi.org/10.1148/rg.242035193>

47. Holshue ML, DeBolt C, Lindquist S et al (2020) Washington State 2019-nCoV case investigation team: Washington State 2019-nCoV case investigation team. First case of 2019 novel coronavirus in the United States. *N Engl J Med* 382:929–936. <https://doi.org/10.1056/NEJMoa2001191>
48. Kanne JP, Little BP, Chung JH, Elicker BM, Ketani LH (2020) Essentials for radiologists on COVID-19: an update-radiology scientific expert panel. *Radiology* 296:E113–E114. <https://doi.org/10.1148/radiol.2020200527>
49. Chan JF, Yuan S, Kok KH et al (2020) A familial cluster of pneumonia associated with the 2019 novel coronavirus indicating person-to-person transmission: a study of a family cluster. *Lancet* 395:514–523. [https://doi.org/10.1016/S0140-6736\(20\)30154-9](https://doi.org/10.1016/S0140-6736(20)30154-9)
50. Müller NL, Ooi GC, Khong PL, Nicolaou S (2003) Severe acute respiratory syndrome: radiographic and CT findings. *AJR Am J Roentgenol* 181:3–8. <https://doi.org/10.2214/AJRAmJRoentgenol.181.1.1810003>
51. Müller NL, Ooi GC, Khong PL, Zhou LJ, Tsang KW, Nicolaou S (2004) High-resolution CT findings of severe acute respiratory syndrome at presentation and after admission. *AJR Am J Roentgenol* 182:39–44. <https://doi.org/10.2214/AJRAmJRoentgenol.182.1.1820039>
52. Chan MS, Chan IY, Fung KH, Poon E, Yam LY, Lau KY (2004) High-resolution CT findings in patients with severe acute respiratory syndrome: a pattern based approach. *AJR Am J Roentgenol* 182:49–56. <https://doi.org/10.2214/AJRAmJRoentgenol.182.1.1820049>
53. Wong KT, Antonio GE, Hui DS et al (2003) Thin-section CT of severe acute respiratory syndrome: evaluation of 73 patients exposed to or with the disease. *Radiology* 228:395–400. <https://doi.org/10.1148/radiol.2283030541>
54. Ajlan AM, Ahyad RA, Jamjoom LG, Alharthy A, Madani TA (2014) Middle East respiratory syndrome coronavirus (MERS-CoV) infection: chest CT findings. *AJR Am J Roentgenol* 203:782–787. <https://doi.org/10.2214/AJRAMJROENTGENOL.14.13021>
55. Das KM, Lee EY, Langer RD, Larsson SG (2016) Middle East respiratory syndrome coronavirus: what does a radiologist need to know? *AJR Am J Roentgenol* 206:1193–1201. <https://doi.org/10.2214/AJRAMJROENTGENOL.15.15363>
56. Koo HJ, Lim S, Choe J, Choi SH, Sung H, Do KH (2018) Radiographic and CT features of viral pneumonia. *RadioGraphics* 38:719–739. <https://doi.org/10.1148/rg.2018170048>
57. Hosseiny M, Kooraki S, Gholamrezanezhad A, Reddy S, Myers L (2020) Radiology perspective of coronavirus disease 2019 (COVID-19): lessons from severe acute respiratory syndrome and Middle East respiratory syndrome. *AJR Am J Roentgenol* 214:1078–1082. <https://doi.org/10.2214/AJRAMJROENTGENOL.20.22969>